National Renewable Energy Laboratory
Innovation for Our Energy Future

A national laboratory of the U.S. Department of Energy
Office of Energy Efficiency & Renewable Energy

Multiblade Coordinate Transformation and Its Application to Wind Turbine Analysis

Preprint

G. Bir

To be presented at the 2008 ASME Wind Energy Symposium
Reno, Nevada
January 7–10, 2008

Conference Paper
NREL/CP-500-42553
January 2008

NREL is operated by Midwest Research Institute • Battelle Contract No. DE-AC36-99-GO10337

Multi-Blade Coordinate Transformation and Its Application to Wind Turbine Analysis

Gunjit Bir[1]
National Renewable Energy Laboratory, Golden, Colorado, 80401

The dynamics of wind turbine rotor blades are generally expressed in rotating frames attached to the individual blades. The rotor, however, responds as a whole to excitations such as aerodynamic gusts, control inputs, and tower-nacelle motion—all of which occur in a nonrotating frame. Similarly, the tower-nacelle subsystem sees the combined effect of all rotor blades, not the individual blades. Multi-blade coordinate transformation (MBC) helps integrate the dynamics of individual blades and express them in a fixed (nonrotating) frame. MBC involves two steps: transformation of the rotating degrees of freedom, and transformation of the equations of motion. This paper details the MBC operation. A new MBC scheme is developed that is applicable to variable-speed turbines, which may also have dissimilar blades. The scheme also covers control, disturbance, output, and feed-forward matrices. Depending on the analysis objective, wind turbine researchers may generate system matrices either in the first-order (state-space) form or the second-order (physical-domain) form. We develop MBC relations for both these forms. MBC is particularly essential for modal and stability analyses. Commonly, wind turbine researchers first compute the periodic state-space matrix, time-average it over the rotor rotational period, and then apply conventional eigenanalysis to compute modal and stability characteristics. Direct averaging, however, eliminates all periodic terms that contribute to system dynamics, thereby producing errors. While averaging itself is not always a bad approach, it must follow MBC. Sample results are presented to illustrate this point and also to show the application of MBC to the modal and stability analysis of a 5-MW turbine.

Nomenclature

A	=	system dynamics matrix
B	=	control matrix for the first-order system
B_d	=	disturbance matrix for the first-order system
b	=	blade number
C	=	matrix consisting of damping and gyroscopic terms
F	=	control matrix for the second-order system
F_d	=	disturbance matrix for the second-order system
K	=	matrix consisting of centrifugal terms and aerodynamic and structural stiffness terms
m	=	the number of rotating degrees of freedom per blade
M	=	mass matrix
nF	=	nonrotating (fixed) degrees of freedom
N	=	number of rotor blades
X	=	physical vector comprising the system degrees of freedom
X_F	=	vector of degrees of freedom for the nonrotating part of the system
X_{NR}	=	vector of system degrees of freedom following MBC
$\widetilde{t}_1, \widetilde{t}_2, \widetilde{t}_3$	=	3x3 transformation matrices, which are functions of the rotor azimuth
T_1, T_2, T_3	=	block-diagonal transformation matrices, which are functions of the rotor azimuth
u	=	control vector
w	=	disturbance vector
Y	=	output vector

[1] NWTC, Mail Stop 3811, 1617, Cole Blvd., AIAA Senior Member.

z	=	state-space vector
q_b	=	bth blade degree of freedom in the rotating frame
Ω	=	rotor angular speed
Ψ	=	reference (1st) blade azimuth
Ψ_b	=	bth blade azimuth
$(\,)_{NR}$	=	a quantity referred to in the nonrotating frame

I. Introduction

The dynamics of wind turbine rotor blades are generally expressed as rotating frames attached to the individual blades. The rotor, however, responds as a whole to excitations such as aerodynamic gusts, control inputs, and tower-nacelle motion—all of which occur in a nonrotating frame. Similarly, the tower-nacelle subsystem sees the combined effect of all rotor blades, not the individual blades. Multi-blade coordinate transformation (MBC) helps integrate the dynamics of individual blades and express it in a fixed (nonrotating) frame. MBC offers several benefits. First, it properly models the dynamic interaction between the nonrotating tower-nacelle and the spinning rotor. Second, it offers physical insight into rotor dynamics and how the rotor interacts with fixed-system entities, such as wind, controls, and tower-nacelle subsystem. Third, MBC filters out all periodic terms except those which are integral multiples of ΩN, where Ω is the rotor angular speed and N is the number of rotor blades. A wind turbine system is basically a periodic system; equations governing its dynamics show periodic parameters, which arise because of the periodic interaction between the rotating subsystem (rotor) and the nonrotating entities (tower, nacelle, wind, controls, and gravity). The blade equations usually contain all harmonics. MBC shows that a rotor behaves as a filter, allowing only specific harmonics of blade motion to be felt by the fixed system. This filtering action also renders the system equations numerically well-conditioned; all nonessential periodic terms are eliminated.

MBC is widely used in the helicopter field. Miller[1] used it to analyze the flap-motion related stability and control. Coleman and Feingold[2] used it to analyze the rotor in-plane motion (lag motion); it was the first successful attempt to understand the helicopter ground resonance problem, which had been eluding the earlier researchers. However, these efforts applied the MBC only in a heuristic fashion. Hohenemser and Yin[3] provided the first mathematically sound basis. Later, Johnson[4] provided a systematic mathematical basis and thorough exposition of the MBC. Using this mathematical basis, Bir et al[5] developed a numerical MBC approach that could be applied to a general helicopter system governed by arbitrary degrees of freedom; the approach was used for stability and response analysis of several helicopters.

Because MBC offers so many benefits, it is receiving attention in the wind turbine field. Bir and Butterfield[6] included MBC in a stability analysis scheme and predicted an instability caused by coalescence between the rotor in-plane and the tower motions. They also showed how MBC provides a physical insight into the rotor in-plane motion. In the turbine field, Malcolm[7] appears to be the first to provide a mathematical form of the turbine equations following application of the MBC. His prime motivation was to relate the inflow characteristics with the turbine response and to extract linearized models from general aeroelastic codes such as ADAMS[8]. McCoy[9] extended this effort to obtain linear time-invariant system equations required in the standard control design approaches. Hansen used MBC for improved modal dynamics to avoid stall-induced vibrations[10] and later combined it with an eigenvalues approach to study the aeroelastic stability characteristics of a three-bladed turbine[11]. Riziotis et al[12] applied MBC to analyze stability of two three-bladed turbines: one stall-regulated and the other pitch-regulated. Bir and Jonkman used MBC in conjunction with FAST [13] to study aeroelastic characteristics of a 5-MW turbine in both land-based and offshore configurations[14].

All attempts at MBC thus far, both in the helicopter and wind turbine fields, have assumed the rotor speed to be constant and the rotor blades to be similar. A modern wind turbine is rarely constant-speed. Also, turbines may not have identical blades, structurally or aerodynamically. We need an MBC approach that overcomes the two limitations.

This paper provides a new MBC scheme that is applicable to a variable-speed turbine, which may also have dissimilar blades. The scheme also covers control, disturbance, output, and feed-forward matrices, which have been ignored to date. Depending on the analysis objective, wind turbine researchers may generate system matrices either in the first-order (state-space) form or the second-order (physical-domain) form. We develop MBC relations for both these forms. In literature, MBC is also referred to as the Fourier coordinate transformation (FCT) and as the Coleman transformation.

Section II describes the MBC operation and how it relates the blade and rotor coordinates. Section III shows how these basic relations are used to transform the system equations of motion from rotating to nonrotating (fixed) coordinates, which is the objective of MBC. We present the two possible approaches to MBC transformation, the substitution method and the operational method, and explain why the substitution method is better suited to numerical analysis. To demonstrate the application of MBC, we chose a conceptual 5-MW, three-blade, upwind wind turbine[15]. Section IV brief describes the properties of this turbine. Though MBC has several applications, it is essential to and mostly used for modal and stability analyses. Commonly, wind turbine researchers first compute the periodic state-space matrix, time-average it over the rotor rotational period, and then apply conventional eigenanalysis to compute modal and stability characteristics. The averaging, however, eliminates all periodic terms that contribute to system dynamics and can cause erroneous results. While averaging itself is not a bad approach, it must follow MBC (Strictly, a Floquet analysis—not averaging—must follow MBC). Section V presents sample results that show how MBC is essential to correct stability analysis.

II. MBC: Transformation of Coordinates

Generally, the turbine equations (i.e., the coupled tower-nacelle-rotor equations) are derived using mixed degrees of freedom, some of which may be in the rotating frame and the other in the nonrotating frame. This is sometimes desirable. For example, in some simulations studies, we may be interested in studying the tower response in the ground-fixed (nonrotating) frame and the blades response in their respective rotating frames. Often, however, we are interested in understanding the coupled behavior of tower-nacelle-rotor system. In such cases, it is desirable to express the full system behavior in a fixed frame. MBC helps us achieve this through a rotating-frame to nonrotating-frame coordinate transformation.

Consider a rotor with N blades that are spaced equally around the rotor azimuth. In such a case, the azimuth location of bth blade is given by

$$\psi_b = \psi + (b-1)\frac{2\pi}{N} \qquad (1)$$

where ψ is the azimuth of the first (reference) blade. We assume that $\psi = 0$ implies the first blade is vertically up. Let q_b be a particular rotating degree of freedom for the bth blade. The MBC is a linear transformation that relates the rotating degrees of freedom to new degrees of freedom defined as follows [4]:

$$\begin{aligned} q_0 &= \frac{1}{N}\sum_{b=1}^{N} q_b \\ q_{nc} &= \frac{2}{N}\sum_{b=1}^{N} q_b \cos n\psi_b \\ q_{ns} &= \frac{2}{N}\sum_{b=1}^{N} q_b \sin n\psi_b \\ q_{N/2} &= \frac{1}{N}\sum_{b=1}^{N} q_b (-1)^b \end{aligned} \qquad (2)$$

These new degrees of freedom are in the nonrotating (fixed) frame. In literature, these are called nonrotating degrees of freedom; we call these rotor coordinates because they express the cumulative behavior of all rotor blades (and not individual blades) in the fixed frame. The physical interpretation of each rotor coordinate depends on the degree of freedom it refers to. For example, if q_b is a flap degree of freedom, then q_0 is the rotor coning, q_{1c} is the rotor tip-path-plane fore-aft tilt about an axis that is horizontal and normal to the rotor shaft, and q_{1s} is the rotor tip-path-plane side-side tilt about an axis that is vertical and normal to the rotor shaft. If q_b is a lag degree of freedom, then q_0 is the rotor collective lag, q_{1c} is the horizontal displacement of the rotor center-of-mass in the rotor plane, and q_{1s} is the vertical displacement of the rotor center-of-mass in the rotor plane [6]. Other degrees of freedom may be interpreted using equations (3) and drawing supporting sketches. The rotor modes corresponding to q_{nc} and q_{ns} ($n>1$) and $q_{N/2}$ are called reactionless modes because they do not cause any transference of moments or forces from the rotor to the hub (fixed frame). The value of n goes from *1* to *(N-1)/2* if N is odd, and from *1* to *(N-2)/2* if N is even. The $q_{N/2}$ mode, called the differential mode, exists only if the number of blades is even.

Most of the wind turbines in the world are three-bladed. Therefore, we will assume *N* to be *3* in the rest of this paper. The formulation developed in the paper for *N=3*, however, is general and can be readily extended for more blades. Setting *N=3* in equations (2), we obtain

$$q_0 = \frac{1}{3}\sum_{b=1}^{3} q_b$$

$$q_c = q_{1c} = \frac{2}{3}\sum_{b=1}^{3} q_b \cos\psi_b \qquad (3)$$

$$q_s = q_{1s} = \frac{2}{3}\sum_{b=1}^{3} q_b \sin\psi_b$$

We will call q_{1c} the cosine-cyclic mode and q_{1s} the sine-cyclic mode. These two cyclic modes, together with the coning mode, q_0, lead to coupling of the rotor with the rest of the turbine. Equations (3) determine the rotor coordinates, given the blade coordinates. The inverse transformation, yielding the blade coordinate given the rotor coordinates, is

$$q_b = q_0 + q_c \cos\psi_b + q_s \sin\psi_b; \quad b = 1,2,3 \qquad (4)$$

III. MBC: Transformation of Equations of Motion

Most aeroelastic codes generate linear equations in the second-order form and, if required (for controls, for example), transform these to a first-order form. We derive MBC relations for both the second- and first-order systems.

A. Second-Order System Equations

Second-order system equations may be written as

$$M\ddot{X} + C\dot{X} + KX = Fu + F_d w \qquad (5a)$$

The associated output equations are

$$Y = C_v\dot{X} + C_d X + Du + D_d w \qquad (5b)$$

where *M, C, K, F,* and F_d are respectively the mass, damping, stiffness, control, and disturbance matrices. The *u* and *w* are respectively the control and disturbance vectors. Note that the C matrix contains gyroscopic terms in addition to the structural damping terms, even though we designate it as a damping matrix. Similarly, K contains centrifugal terms in addition to the structural and aerodynamic stiffness terms. Also, each of these matrices contains direct and cross-coupling terms. For example, *M* contains direct blade inertias as well as blade-tower coupling inertias. However, the formulation we develop does not require a user to explicitly partition any of the matrices into sub-matrices delineating direct and cross-coupling terms. The partitioning is implicit in the definition of the coordinates vector *X* (also called the physical vector in literature). Assume that *X* is expressed as

$$X = \begin{Bmatrix} X_F \\ q_1^1 \\ q_2^1 \\ q_3^1 \\ \vdots \\ q_1^j \\ q_2^j \\ q_3^j \\ \vdots \\ q_1^m \\ q_2^m \\ q_3^m \end{Bmatrix} \qquad (6)$$

where X_F is a $nF \times 1$ column vector representing the nF fixed-frame-referenced degrees of freedom and q_b^j is the j^{th} rotating degree of freedom for the b^{th} blade. As is evident from (6), m is the number of rotating degrees of freedom for each blade. Thus the length of vector X is $nF+3m$, the total number of degrees of freedom for the full system. Most often, aeroelastic codes assume that the physical vector has the form (6). If not, we can always perform simple rows and columns exchange to transform system equations (5) such that the physical vector X assumes the form (6).

There are two methods to transform equations (5) to the nonrotating frame: the operational method and the substitution method. In the operational method, we apply the following summation operators to the rotating-frame equations of motion:

$$\begin{aligned} &\frac{1}{3}\sum_{b=1}^{3}(rot\_eqns) \\ &\frac{2}{3}\sum_{b=1}^{3}(rot\_eqns)\cos\psi_b \\ &\frac{2}{3}\sum_{b=1}^{3}(rot\_eqns)\sin\psi_b \end{aligned} \qquad (7)$$

where *rot-eqns* refers to the rotating-frame equations of motion. Note the similarity of summation operators in equations (3) and (7). To accomplish these operations, we first need that the *rot-eqns* are available in an analytical form showing all periodic terms explicitly; the periodic terms involve trigonometric functions of $\sin(k\Psi_b)$ and $\cos(k\Psi_b)$ terms, where k in general can have any integer value depending on the system. First, we must express all products of trigonometric functions as sums of trigonometric functions. Next, we must perform cumbersome operations to ensure that the value of each n in these trigonometric functions satisfies the requirements of equations (3). Finally, we use transformation (3) to convert the *rot-eqns* to the nonrotating frame. The operational method is thus quite tedious and applicable only if we have equations of motion available in an analytical form.

All aeroelastic codes generate equations of motion in a numerical form and, therefore, are not amenable to the operational method. We must instead use the substitutional method. In this method, we substitute the rotational degrees of freedom with the rotor coordinate using equation (4). If we do so, the three rotational degrees of freedom (q_1^j, q_2^j, q_3^j), corresponding to the jth degree of freedom for each of the three blades, may be transformed to nonrotating coordinates (q_0^j, q_c^j, q_s^j) using the following relation:

$$\begin{Bmatrix} q_1^j \\ q_2^j \\ q_3^j \end{Bmatrix} = \tilde{t} \begin{Bmatrix} q_0^j \\ q_c^j \\ q_s^j \end{Bmatrix} \qquad (8)$$

where

$$\tilde{t} = \begin{bmatrix} 1 & \cos\psi_1 & \sin\psi_1 \\ 1 & \cos\psi_2 & \sin\psi_2 \\ 1 & \cos\psi_3 & \sin\psi_3 \end{bmatrix} \tag{9}$$

Using (8), the full-system rotating-frame degrees-of-freedom vector, X, is expressed in terms of the nonrotating-frame degrees-of-freedom vector, X_{NR}, as follows

$$X = T_1 X_{NR} \tag{10}$$

where T_1 is the block diagonal matrix:

$$T_1 = \begin{bmatrix} I_{nF\times nF} & & & & \\ & \tilde{t} & & & \\ & & \tilde{t} & & \\ & & & \ddots & \\ & & & & \tilde{t} \end{bmatrix}_{(nF+3m)\times(nF+3m)} \tag{11}$$

and

$$X_{NR} = \begin{Bmatrix} X_F \\ q_0^1 \\ q_c^1 \\ q_s^1 \\ \vdots \\ q_0^j \\ q_c^j \\ q_s^j \\ \vdots \\ q_0^m \\ q_c^m \\ q_s^m \end{Bmatrix} \tag{12}$$

Taking the first and second time derivatives of the two sides of equation (10), we obtain

$$\begin{aligned} \dot{X} &= T_1\dot{X}_{NR} + \Omega T_2 X_{NR} \\ \ddot{X}_{NR} &= T_1\ddot{X}_{NR} + 2\Omega T_2\dot{X}_{NR} + (\Omega^2 T_3 + \dot{\Omega} T_2) X_{NR} \end{aligned} \tag{13}$$

where $\boldsymbol{\Omega}$ is the rotor angular velocity and $\dot{\Omega}$ is the rotor angular acceleration. The T_2 and T_3 transformation matrices are given by

$$T_2 = \begin{bmatrix} 0_{nF\times nF} & & & & \\ & \tilde{t}_2 & & & \\ & & \tilde{t}_2 & & \\ & & & \ddots & \\ & & & & \tilde{t}_2 \end{bmatrix}_{(nF+3m)\times(nF+3m)} \tag{14}$$

$$T_3 = \begin{bmatrix} 0_{nF\times nF} & & & \\ & \tilde{t}_3 & & \\ & & \tilde{t}_3 & \\ & & & \ddots \\ & & & \tilde{t}_3 \end{bmatrix}_{(nF+3m)\times(nF+3m)} \tag{15}$$

where

$$\tilde{t}_2 = \begin{bmatrix} 0 & -\sin\psi_1 & \cos\psi_1 \\ 0 & -\sin\psi_2 & \cos\psi_2 \\ 0 & -\sin\psi_3 & \cos\psi_3 \end{bmatrix} \quad and \quad \tilde{t}_3 = \begin{bmatrix} 0 & -\cos\psi_1 & -\sin\psi_1 \\ 0 & -\cos\psi_2 & -\sin\psi_2 \\ 0 & -\cos\psi_3 & -\sin\psi_3 \end{bmatrix} \tag{16}$$

Substituting for X and its time derivatives from equations (10) and (13) in equations (5a) and (5b), we obtain the system equations of motion in the nonrotating frame as

$$M_{NR}\ddot{X}_{NR} + C_{NR}\dot{X}_{NR} + K_{NR}X_{NR} = F_{NR}u_{NR} + F_{d\,NR}w \tag{17}$$

and

$$Y_{NR} = C_{v\,NR}\dot{X}_{NR} + C_{d\,NR}X_{NR} + D_{NR}u_{NR} + D_{d\,NR}w \tag{18}$$

The subscript NR identifies the associated quantity to be in the nonrotating frame. The various matrices appearing in equations (17) and (18) are as follows

$$\begin{aligned} M_{NR} &= MT_1 \\ C_{NR} &= 2\Omega MT_2 + CT_1 \\ K_{NR} &= \Omega^2 MT_3 + \dot{\Omega}MT_2 + \Omega CT_2 + KT_1 \\ F_{NR} &= FT_{1c} \\ F_{d\,NR} &= F_d \\ C_{v\,NR} &= T_{1o}^{-1}C_vT_1 \\ C_{d\,NR} &= T_{1o}^{-1}(\Omega C_vT_2 + C_dT_1) \\ D_{NR} &= T_{1o}^{-1}DT_{1c} \\ D_{d\,NR} &= T_{1o}^{-1}D_d \end{aligned} \tag{19}$$

Note that the variable-speed operation affects only the stiffness matrix. Also, the disturbance matrix stays unchanged; this is because the disturbance w is already in the nonrotating frame. If Fc and mc are the number of controls in the fixed and rotating frames respectively, then the control vectors u and u_{NR} are related as follows:

$$u = T_{1c}u_{NR} \tag{20}$$

where

$$T_{1c} = \begin{bmatrix} I_{FcxFc} & & & \\ & \tilde{t} & & \\ & & \tilde{t} & \\ & & & \ddots \\ & & & \tilde{t} \end{bmatrix}_{(Fc+3mc)X(Fc+3mc)} \tag{21}$$

Similarly,

$$Y = T_{1o}Y_{NR} \tag{22}$$

where

$$T_{1o} = \begin{bmatrix} I_{FoxFo} & & & & \\ & \tilde{t} & & & \\ & & \tilde{t} & & \\ & & & \ddots & \\ & & & & \tilde{t} \end{bmatrix}_{(Fo+3mo)X(Fo+3mo)} \tag{23}$$

where *Fo* and *mo* are the number of outputs in the fixed and rotating frames respectively. In summary, following the application of MBC, the rotating-frame second-order equations (5a) and (5b) are transformed to the nonrotating-frame equations (17) and (18).

B. First-Order System Equations

First-order system equations are generally expressed as

$$\dot{z} = Az + Bu + B_d w \tag{24}$$

where z is the state-space vector. The A, B, and B_d are respectively the system dynamics, control, and disturbance matrices. The u and w are the control and disturbance vectors. The associated output equations are

$$Y = Cz + Du + D_d w \tag{25}$$

The state-space vector, z, is related to the physical vector, X, as follows:

$$z = \begin{Bmatrix} X \\ \dot{X} \end{Bmatrix} \tag{26}$$

Using equations (26) , (8-16) and (20-23), equations (24) and (25) are transformed to the nonrotating frame as follows:

$$\dot{z}_{NR} = A_{NR} z_{NR} + B_{NR} u_{NR} + B_{d\,NR} w \tag{27}$$

and

$$Y_{NR} = C_{NR} z_{NR} + D_{NR} u_{NR} + D_{d\,NR} w \tag{28}$$

The subscript *NR* identifies the associated quantity to be in the nonrotating frame. The various matrices appearing in equations (27) and (28) are as follows

$$A_{NR} = \begin{bmatrix} T_1^{-1} & 0 \\ 0 & T_1^{-1} \end{bmatrix} \left\{ A \begin{bmatrix} T_1 & 0 \\ \Omega T_2 & T_1 \end{bmatrix} - \begin{bmatrix} \Omega T_2 & 0 \\ \Omega^2 T_3 + \dot{\Omega} T_2 & 2\Omega T_2 \end{bmatrix} \right\} \tag{29}$$

$$B_{NR} = \begin{bmatrix} T_1^{-1} & 0 \\ 0 & T_1^{-1} \end{bmatrix} B T_{1C} \tag{30}$$

$$C_{NR} = T_{10}^{-1} \begin{bmatrix} C_1 T_1 + \Omega C_2 T_2 & C_2 T_1 \end{bmatrix}; \quad C = \begin{bmatrix} C_1 & C_2 \end{bmatrix} \tag{31}$$

$$D_{NR} = T_{10}^{-1} D T_{1C} \tag{32}$$

$$D_{d\,NR} = T_{10}^{-1} D_d \tag{33}$$

In summary, following the application of MBC, the rotating-frame first-order equations (24) and (25) are transformed to the nonrotating-frame equations (27) and (28). Also, note that the dynamics matrix, A, is influenced by the variable rotor speed.

C. Misconceptions About MBC

Certain misconceptions regarding MBC frequently arise both in the helicopter and the wind energy fields. The main ones are:

1) The rotor must spin at a constant speed.
2) MBC transforms a time-variant system to a time-invariant one.
3) The rotor blades must have identical structural and aerodynamic properties.

None of the above statements is true. Explanatory remarks follow:

1) In the previous section, we derived MBC relations assuming that the rotor speed, **Ω,** varies. MBC is thus applicable to variable-speed turbines.
2) MBC does not eliminate all periodic terms, thereby transforming a time-variant system to a time-invariant one. MBC actually acts as a filter; it lets through terms that are integral multiples of ΩN and filters out the rest the other periodic terms, provided all blades are identical and the operating conditions are time-invariant.
3) In deriving the MBC relations, we never assumed the rotor blades to be identical, structurally or aerodynamically. Any dissimilarity will be reflected in the system matrices and MBC can be applied to such matrices. For dissimilar blades, however, MBC will not be able to filter out even those periodic terms that are not integral multiples of Ω*N*.

The only restriction for MBC to be applicable is that the blades be spaced equally around the rotor azimuth.

Another misconception (related to the second misconception listed above) is that Floquet analysis is not required if MBC is applied. Because MBC does not eliminate all periodic terms, a Floquet[4,16] analysis is required, particularly if the blades are dissimilar.

IV. Brief Description of the 5-MW Wind Turbine

The conceptual wind turbine used for stability analysis in this paper consists of an upwind, three-bladed, 126-meter diameter rotor mounted on top of an 87.6-meter tower. Jonkman et al [15] selected its properties so as to best match a few existing 5-MW designs. Salient turbine properties are summarized in Table 1; other properties can be found in the cited reference. The NREL offshore 5-MW baseline wind turbine has been used to establish the reference specifications for a number of research projects supported by the U.S. Department of Energy's Wind Energy Technologies Program.

Table 1. Summary of Baseline Wind Turbine Properties

Rating	5 MW
Rotor Orientation	Upwind
Control	Variable Speed, Collective Pitch
Rotor Diameter	126 m
Hub Height	90 m
Cut-In, Rated, Cut-Out Wind Speed	3 m/s, 11.4 m/s, 25 m/s
Cut-In, Rated Rotor Speed	6.9 rpm, 12.1 rpm
Rated Tip Speed	80 m/s
Overhang, Shaft Tilt, Precone	5 m, 5°, 2.5°
Blade Structural Damping Ratio	2.5%
Tower Structural Damping Ratio	1.0%

V. Results: Application of MBC to Stability Analysis

For stability analysis, we consider two sets of operating conditions: parked conditions and normal operating conditions. In the parked condition, the generator torque is assumed to be zero, implying that the rotor is free to idle. All results are obtained using a structural damping ratio of 1% for the tower and 2.5% for the blades. Because the linearization scheme in FAST cannot yet handle active controls and dynamic stall, we ignore these effects during stability analyses.

A. Parked Condition

We analyzed stability characteristics of the 5-MW turbine for a number of parked conditions, which are mandated by the International Electrotechnical Commission (IEC) design standard[17,18]. However, to illustrate the importance of MBC, we present results for only one parked condition covered under the IEC load case 6.2a. Due to loss of grid, the turbine is free to idle. It encounters an extreme 50 m/s wind with the nacelle yaw set at 140^0 with respect to the wind direction. All blades are feathered at 90^0. Under these conditions, trim analysis using FAST predicts that the rotor would idle at an angular speed of 0.0076 Hz. Using this rotor speed, we again used FAST to generate the system dynamic matrix, *A*. (see equation 24). Next, we used two approaches to compute the stability characteristics.

In the first approach, we azimuth-averaged the system matrix A and then computed its eigensolution. Eigenvalues provided the modal damping and frequencies; eigenvectors helped us identify the modes. Table 2 lists the modal dampings. A negative damping, identified in bold red, implies instability.

In the second approach, we first performed MBC to obtain A_{NR}. Then we azimuth-averaged the matrix A_{NR} and computed its eigensolution. The third column in Table 2 lists the predicted modal dampings.

Table 2. Modal Damping Ratios (nacelle yaw =140^0; all blades pitched at 90^0)

Mode	Damping ratio (%)	
	Without MBC	With MBC
1st lag	0.21628	**-0.26399**
1st flap	0.64873	2.5098
2nd flap	0.27054	2.0333
tower 1st side-to-side	**-0.58981**	2.1163
tower 1st fore-aft	0.97208	2.7269
tower 2nd side-side	0.80674	3.0489
tower 2nd fore-aft	0.76662	3.9751

We see that the two approaches not only yield different damping predictions, but can also lead to erroneous conclusions. If MBC is not used, instability might be interpreted as stability and vice versa. The reason is simple. In the first approach, direct averaging eliminates all periodic terms that contribute to system dynamics, therefore, erroneous results follow. In the second approach, the MBC is applied first; this appropriately transforms the periodic terms and also filters out the nonessential periodicity. Results are, therefore, improved. While averaging itself is not a bad approach, it must follow MBC (strictly, a Floquet analysis—not averaging—must follow MBC).

B. Normal Operating Condition

As is done in a typical stability analysis, we first obtain modal frequencies versus the rotor speed when the rotor is spinning in vacuum. These frequencies and associated modes offer insight into system dynamics and help interpret the stability modes. The results are obtained using MBC followed by eigenanalysis. This plot of modal frequencies versus the rotor speed, usually called the Coleman diagram, is shown in Fig.1.

A consequence of the MBC transformation, described in Section III, is that the individual *blade* modes are transformed to *rotor* modes. Consider the first lag (edgewise) mode of each blade. Instead of seeing three first lag modes, one for each blade, we see three rotor modes: Lag 1_coll, Lag 1_prog, and Lag 1_reg. These modes are respectively the first-lag collective, progressive, and regressive modes and are physically more meaningful. Note that the tower-nacelle-drivetrain system sees the cumulative effect of all blades and not the individual blades. The rotor modes in fact represent the cumulative effect of all the blades. The collective lag mode is a rotor mode in which all the blades bend, within the rotor plane, in the same direction (either clockwise or counterclockwise) and with the same magnitude and phase. One can visualize that this rotor mode would interact with the drivetrain torsion mode. In the other two lag modes, the blades oscillate within the plane of the rotor in such a way that the effective center of mass of the rotor whirls about the rotor shaft. In the progressive mode, the center of mass whirls in the *same* direction as the rotor spin direction but at an angular speed *higher* than the rotor speed. In the regressive mode, the center of mass whirls in a direction *opposite* to that of the rotor spin and at an angular speed *lower* than the rotor speed. One can visualize that the mass imbalance associated with the rotor center-of-mass whirl can induce whirling of the rotor shaft bending mode and to some extent the tower bending mode. FAST, however, cannot yet model the shaft bending and, therefore, our results do not show any drivetrain whirl.

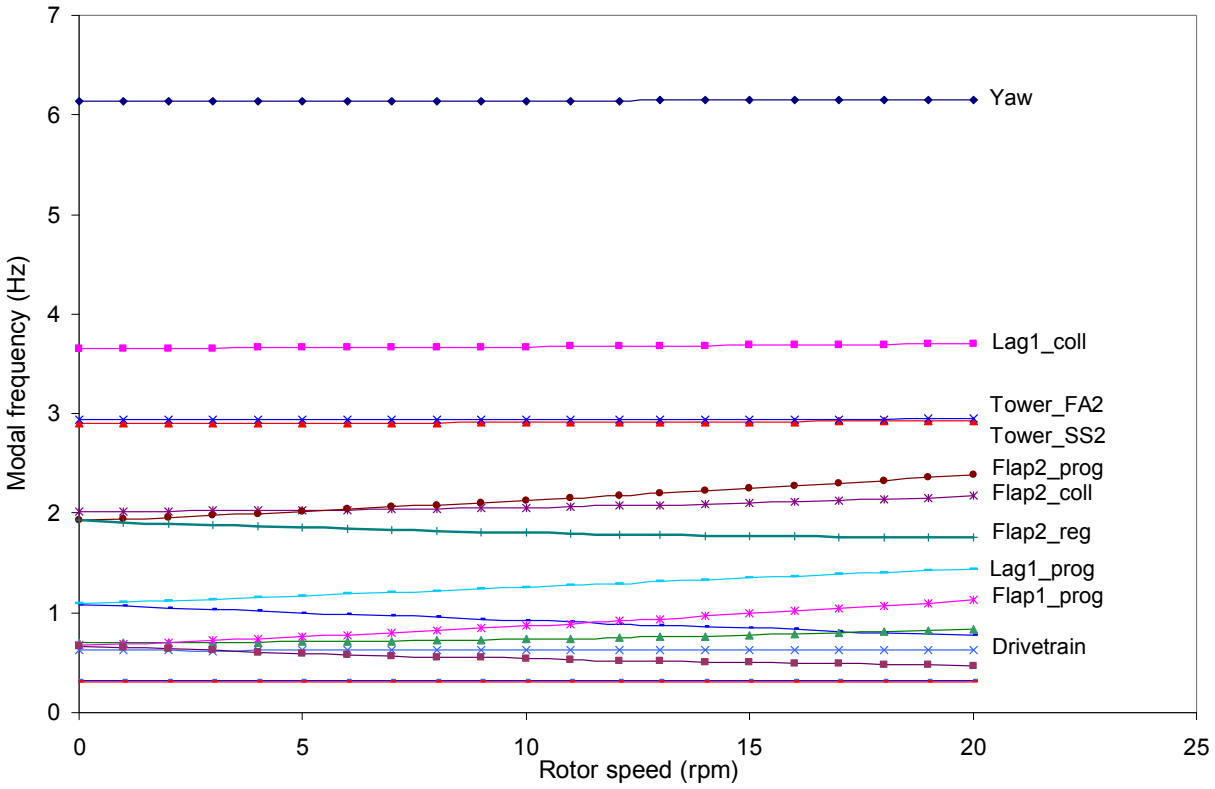

Figure 1. Variation of in-vacuum modal frequencies with rotor speed (Coleman diagram).

As with the lag modes, the rotor exhibits flap modes that represent the cumulative effect of all the blades. Each mode, however, has a different physical significance and interacts differently with the fixed (tower-nacelle) system. The collective flap mode is a rotor mode in which all the blades flap, out of the rotor plane, in unison and with the same magnitude. One can visualize that in this mode, the rotor cones back and forth and interacts with the tower fore-aft mode. In the progressive flap mode, the rotor disk wobbles in the *same* direction as the rotor spin direction and at an angular speed *higher* than the rotor speed. In the regressive flap mode, the rotor disk wobbles in a direction *opposite* to that of the rotor spin direction and at an angular speed *lower* than the rotor speed.

In Fig. 1, we note that the nacelle yaw frequency, around 6.1 Hz, is hardly influenced by the rotor speed as expected. The variation of other frequencies is difficult to discern in this figure. Therefore, the results are replotted in Fig. 2. Note that the tower's second side-to-side (Tower_SS2) modal frequency increases somewhat with rotor speed; this is due to its coupling with the second flap collective mode, which stiffens centrifugally as the rotor speed increases. Because of centrifugal stiffening, the frequencies of other collective modes (Flap1_coll and Lag1_coll) also increase with rotor speed. The frequencies of all progressive modes also increase with rotor speed. Note, however, that the progressive mode frequencies increase at rates much higher than those of the corresponding collective modes. All regressive mode frequencies decrease with rotor speed.

Readers familiar with the isolated rotor modes, wherein the tower-nacelle subsystem is fully rigid, will notice interesting differences. For an isolated rotor, progressive and regressive modal frequency curves are symmetric about the corresponding collective modal frequency curve; at any rotor speed, Ω, the progressive mode frequency is $\omega\_coll + \Omega$, and the regressive mode frequency is $\omega\_coll - \Omega$, where ω_coll is the collective mode frequency. However, this symmetry is lost for the full system because different rotor modes interact differently with the tower-nacelle subsystem. Even more interestingly, the Lag1_coll frequency curve is not even located between the Lag1_prog and Lag1_reg curves, normally observed for an isolated rotor. This is because the first rotor lag collective mode strongly interacts with the torsionally compliant drivetrain mode. The drivetrain mode frequency itself, however, is unaffected by the rotor speed. A more in-depth discussion of modal interaction amongst several subsystems is not in the scope of this paper.

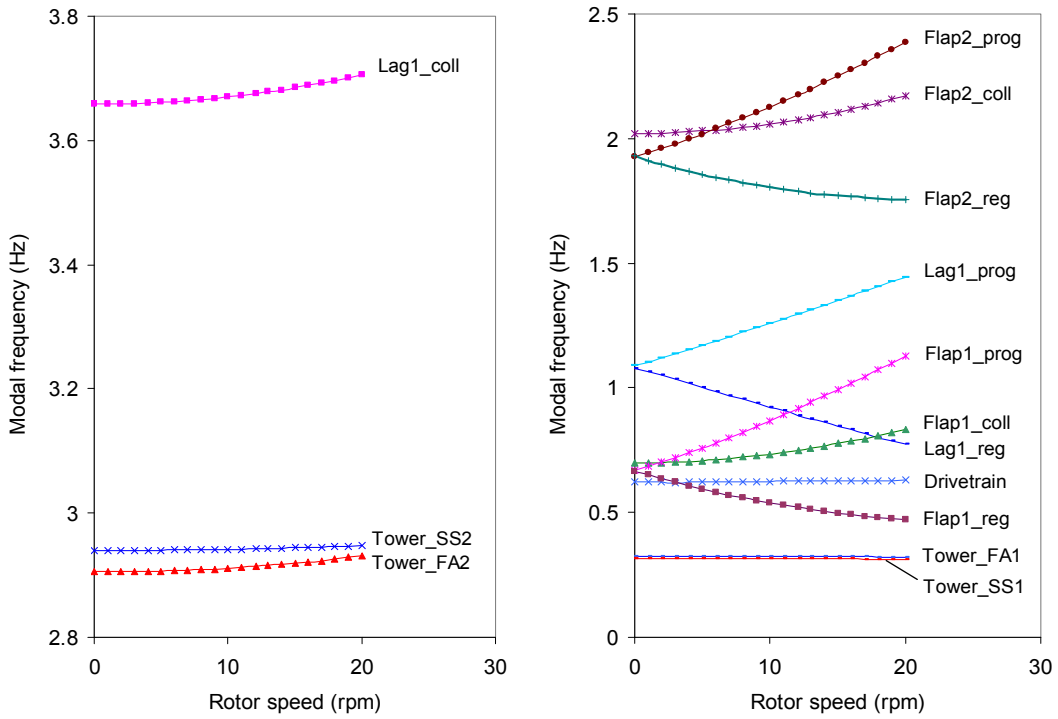

Figure 2. Variation of in-vacuum modal frequencies with rotor speed (land-based configuration).

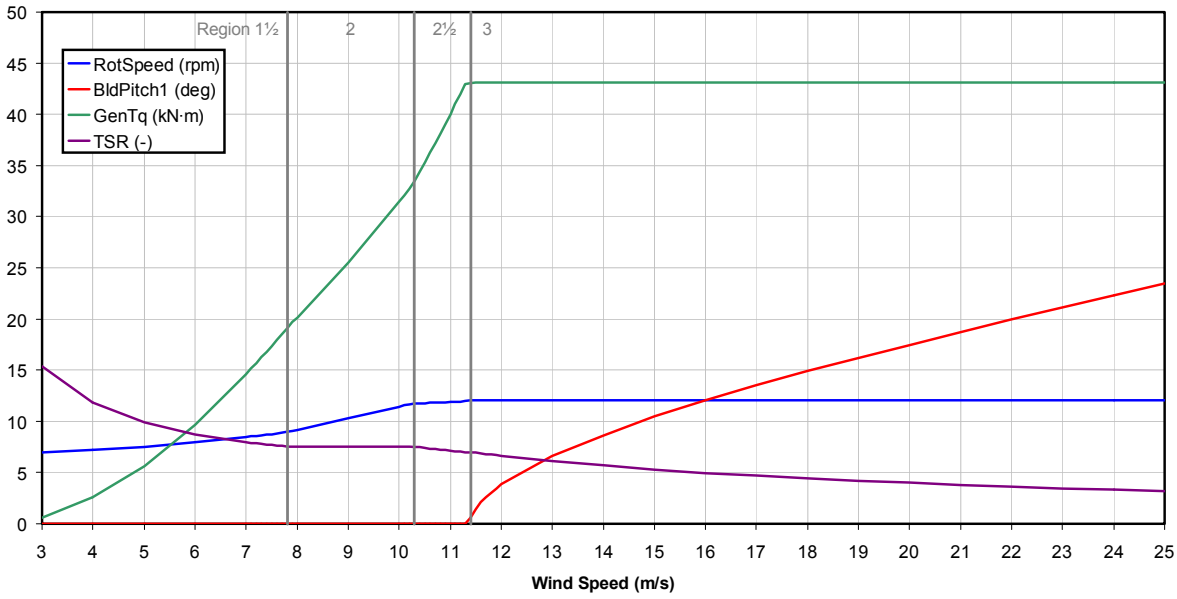

Figure 3. Variations of controlled blade-pitch angle and rotor speed with wind speed.

Now we consider turbine normal operation in the presence of wind. The wind speed varies from 3 m/s (cut-in speed) to 25 m/s (cut-out speed). For a given wind speed, each blade's pitch and rotor speed are set to the values depicted in Fig. 3. These values ensure optimum performance in region 2 and power regulation in region 3 [15]. Stability analysis results are presented in Figs. 4 and 5.

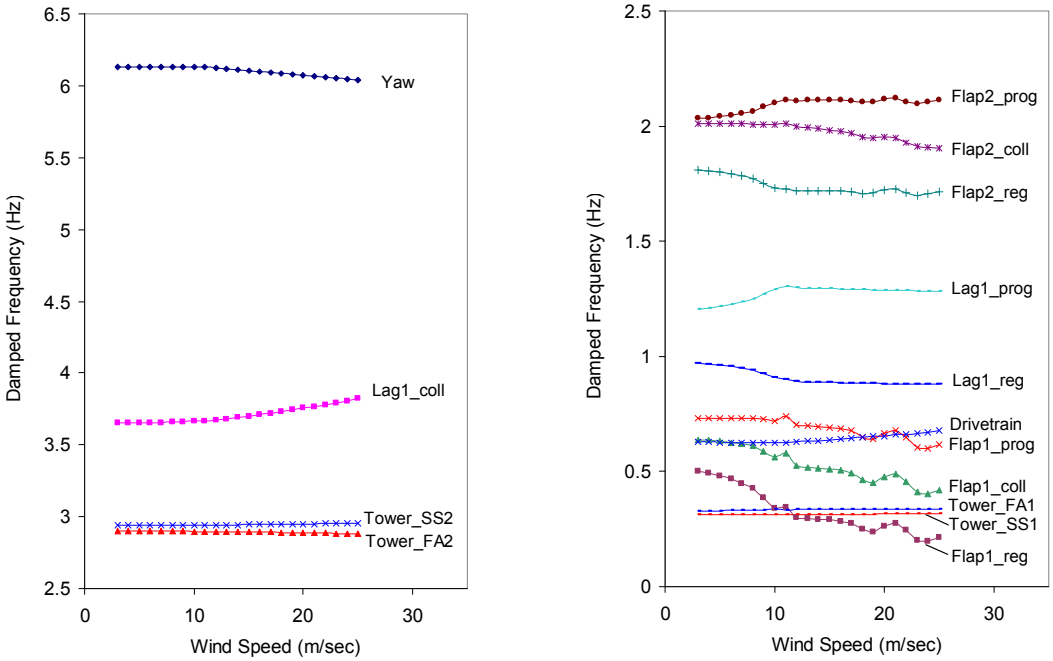

Figure 4. Variations of damped modal frequencies with wind speed (land-based configuration).

Figure 4 shows the variation of damped modal frequencies with wind speed. The exact physics behind the various modal frequency trends is still under investigation. However, we make a few observations. Frequencies of the nacelle yaw, Flap2_coll, and Flap1_coll, and Flap1_prog modes decrease with wind speed, indicating a strong influence of aeroelastic couplings. A sudden change in the frequency trends near 11 m/s wind speed is due to the fact that the rotor speed is held constant beyond this wind speed (see Fig. 3). The cause behind the erratic behavior of some frequency curves beyond the 22 m/s wind speed is still to be examined. Note that all tower modes are relatively insensitive to the wind speed.

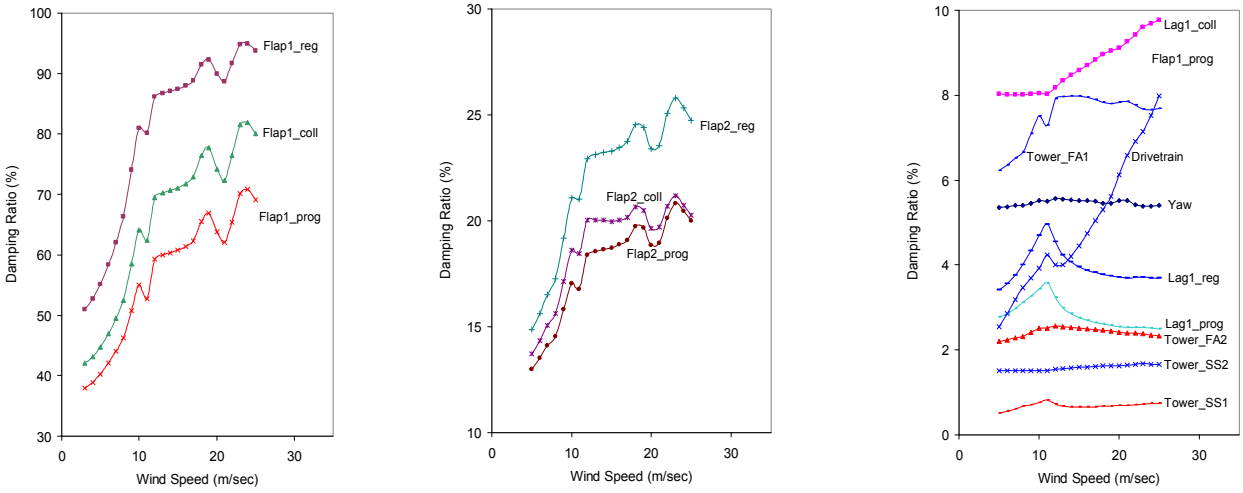

Figure 5. Variations of modal damping ratios with wind speed (land-based configuration).

Figure 5 shows the variation of modal damping ratios with wind speed. All modes have positive damping, implying that they are all stable. As expected, all flap modes are highly damped. However, damping of the rotor first flap modes exceeding 50% is somewhat high; in our experience with typical rotors, this damping is in the range 30%–50%. This suggests that the blade is quite light in comparison to its aerodynamic capability. Typical blades have a Lock number in the range 8–10 (a Lock number is a nondimensional parameter that expresses the aerodynamic lift capability of a blade in comparison to its weight [4]). The blade in this study has an effective Lock

number of about 12. Damping of both the progressive and regressive lag modes increases rapidly as wind speed is increased from 3 m/s to about 11 m/s; thereafter it decreases and becomes almost constant beyond the wind speed of 22 m/s. The drivetrain frequency increases monotonically except near a wind speed of 12 m/s where it shows a slight dip. The tower first side-to-side mode is the least damped showing maximum damping of about 0.8%.

VI. Conclusions

A new multiblade coordinate transformation (MBC) scheme is presented that is applicable to both constant- and variable-speed turbines; it also allows dissimilar blades. The scheme covers control, disturbance, and output-related matrices, which are often required by control designers. Equations governing MBC are developed for both the first- and the second-order systems. Next, we showed that the common approach of first time-averaging the system matrices over the rotor azimuth and then applying eigenanalysis can lead to erroneous modal and stability predictions. Direct averaging eliminates all periodic terms that contribute to system dynamic; therefore causing erroneous results. While averaging itself is not a bad approach, it must follow MBC. Finally, we showed application of MBC to the modal and stability analysis of a 5-MW turbine.

Though the MBC formulation developed in this paper assumes a three-bladed turbine, the formulation is general enough to be readily extendable to a turbine with more than three blades. We plan to do so in the future.

Acknowledgments

Thanks to Sandy Butterfield from NREL for motivating this effort, to Jason Jonkman for providing the 5-MW turbine data, and to Kathy O'Dell for editing this paper. This work was performed in support of the U.S. Department of Energy under contract number DE-AC36-83CH10093.

References

[1]Miller, R. H., "Helicopter control and stability in hovering flight," *JAS* , 15:8, August 1948.

[2]Coleman, R. P. and Feingold, A. M., "Theory of self-excited mechanical oscillations of helicopter rotors with hinged blades," *NACA Technical Report TR 1351*, 1958.

[3]Hohenemser, K. H. and Yin, S. K., "Some applications of the method of multiblade coordinates," *Journal of the American Helicopter Society* , Vol. 17, No. 3, July 1972.

[4]Johnson, W., *Helicopter Theory*. Princeton University Press, New Jersey, 1980.

[5]Bir, G., Chopra, I., et al. "University of Maryland Advanced Rotor Code (UMARC) Theory Manual," Technical Report UM-AERO 94-18, Center for Rotorcraft Education and Research, University of Maryland, College Park, July 1994.

[6]Bir, G.S., Wright, A.D. and Butterfiled, S., "Stability Analysis of Variable-Speed Wind Turbines", Proceedings of the 1997 ASME Wind Energy Symposium, Reno, January 6-9, 1997.

[7]Malcolm, D. J., "Modal Response of 3-Bladed Wind turbines," *Journal of Solar Engineering*, Vol. 124, No. 4, Nov. 2002, pp. 372-377.

[8]Elliott, A.S.; McConville, J.B. (1989). "Application of a General-Purpose Mechanical Systems Analysis Code to Rotorcraft Dynamics Problems." Presented at the American Helicopter Society National Specialists' Meeting on Rotorcraft Dynamics, 1989.

[9]McCoy, T. J., "Wind turbine ADAMS model linearization including rotational and aerodynamic effects," *2004 ASME Wind Energy Symposium*, Jan. 2004, pp. 224-233.

[10]Hansen, M. H., "Improved modal dynamics of wind turbines to avoid stall-induced vibrations," *Wind Energy*, Vol. 6, Issue 2, 2003, pp.179-195.

[11]Hansen, M. H., "Stability analysis of three-bladed turbines using an eigenvalue approach," *2004 ASME Wind Energy Symposium*, Jan. 2004, pp. 192-202.

[12]Riziotis, V. A., Voutsinas, S. G., Politis, E. S., and Chaviaropoulos, P. K., "Aeroelastic stability of wind turbines: The problem, the methods, and the issues," *Wind Energy*, Vol. 7, Issue 4, 2004, pp.373-392.

[13]Jonkman Jonkman, J. M. and Buhl, M. L., Jr., "FAST User's Guide," NREL/EL-500-29798, Golden, CO: National Renewable Energy Laboratory, October 2004.

[14]Bir, G. and Jonkman, J., "Aeroelastic instabilities of large offshore and onshore wind turbines," *Journal of Physics: Conference Series*, 2007.

[15] Jonkman, J.; Butterfield, S.; Musial, W.; and Scott, G., "Definition of a 5-MW Reference Wind Turbine for Offshore System Development," NREL/TP-500-38060, Golden, CO: National Renewable Energy Laboratory, February 2007 (to be published).

[16]Bir, G. and Stol K., "Modal analysis of a teetered-rotor turbine using the Floquet approach," *Proceedings of the AIAA/ASME Wind Energy Symposium*, Jan. 2000.

[17] IEC 61400–1 Ed. 3, *Wind Turbines–Part 1: Design Requirements*, International Electrotechnical Commission (IEC), 2005.

[18] IEC 61400–3, *Wind Turbines – Part 3: Design Requirements for Offshore Wind Turbines*, International Electrotechnical Commission (IEC), 2006 (to be published).

REPORT DOCUMENTATION PAGE

Form Approved
OMB No. 0704-0188

PLEASE DO NOT RETURN YOUR FORM TO THE ABOVE ORGANIZATION.

1. REPORT DATE *(DD-MM-YYYY)*	2. REPORT TYPE	3. DATES COVERED *(From - To)*
January 2008	Conference paper	

4. TITLE AND SUBTITLE
Multiblade Coordinate Transformation and Its Application to Wind Turbine Analysis: Preprint

5a. CONTRACT NUMBER
DE-AC36-99-GO10337

5b. GRANT NUMBER

5c. PROGRAM ELEMENT NUMBER

6. AUTHOR(S)
Bir, G.

5d. PROJECT NUMBER
NREL/CP-500-42553

5e. TASK NUMBER
WER82101

5f. WORK UNIT NUMBER

7. PERFORMING ORGANIZATION NAME(S) AND ADDRESS(ES)
National Renewable Energy Laboratory
1617 Cole Blvd.
Golden, CO 80401-3393

8. PERFORMING ORGANIZATION REPORT NUMBER
NREL/CP-500-42553

9. SPONSORING/MONITORING AGENCY NAME(S) AND ADDRESS(ES)

10. SPONSOR/MONITOR'S ACRONYM(S)
NREL

11. SPONSORING/MONITORING AGENCY REPORT NUMBER

12. DISTRIBUTION AVAILABILITY STATEMENT
National Technical Information Service
U.S. Department of Commerce
5285 Port Royal Road
Springfield, VA 22161

13. SUPPLEMENTARY NOTES

14. ABSTRACT *(Maximum 200 Words)*
Multiblade coordinate transformaton (MBC) modeling integrates the dynamics of individual wind turbine blades and and expresses them as fixed frames. This paper describes MBC modeling and a new MBC scheme developed for variable-speed turbines that may also have dissimilar blades.

15. SUBJECT TERMS
wind turbine; wind turbine blades; wind turbine computer modeling;

16. SECURITY CLASSIFICATION OF:			17. LIMITATION OF ABSTRACT	18. NUMBER OF PAGES	19a. NAME OF RESPONSIBLE PERSON
a. REPORT	b. ABSTRACT	c. THIS PAGE			19b. TELEPHONE NUMBER (*Include area code*)
Unclassified	Unclassified	Unclassified	UL		

Standard Form 298 (Rev. 8/98)
Prescribed by ANSI Std. Z39.18